Carrasco-Sanz, A., Martín-López, S., Corredera, P., González-Herráez, M., Hernanz, M.L., 2006, “High-power and high-accuracy integrating sphere radiometer: Design, characterization, and calibration", Applied Optics, 45, n.3, pp. 511-518.

Available at http://dx.doi.org/10.1364/AO.45.000511

High power integrating sphere radiometer: design, characterization and calibration (400-1700 nm).

Félix Rodríguez-Barrios(1), Ana Carrasco-Sanz(1), Sonia Martín-López(1), Pedro Corredera Guillén(1),
Miguel González-Herráez(1,2) y María Luisa Hernanz Sanjuan(1).

(1) Dept. de Metrología, Instituto de Física Aplicada, CSIC. Serrano 144, 28006, Madrid
(2) Dept. de Electrónica, Escuela Politécnica Superior, Universidad de Alcalá. Campus Universitario, 28871, Alcalá de Henares, Madrid.

***Abstract**: This paper describes the design, characterization and calibration of a high power transfer standard for optical power measurements in fibres based on an integrating sphere radiometer (ISR). This ISR can accurately measure powers between -50 dBm to +40 dBm and, because it uses two different detectors (Si and InGaAs) it is useful in the wavelength range from 400 to 1700 nm.*

The radiometer has been calibrated along the total spectral range of use against an electrically calibrated pyroelectric radiometer and different fibre laser diodes and ion lasers. The total uncertainty obtained is lower than ±1.5% for these wavelength and power ranges.

1.- Introduction.

The proliferation of high power fibre lasers used to pump Raman amplifiers having output powers of several watts, at wavelengths as 1100, 1365, 1420, 1455, 1480 and 1495 nm, and the increasing demand of more precision and better accuracy in the measurement of the fiber nonlinear parameters drives the need to improve the calibration capabilities for absolute power measurements in fibres at levels from 0.5 W to 10 W [1, 2].

Integrating sphere radiometers (ISR) have been demonstrated as a realizable system to develop fibre-optic power meter scales [3, 4, 5], and NIR spectral responsivity scales using a monochromator-based cryogenic radiometers [6] or a laser-based cryogenic radiometer facilities [7].

This paper presents the design, characterization and calibration of an ISR useful in the 400-1650 nm wavelength range. The sphere radiometer has been calibrated at 0 dBm and using the linearity characterization of Si and InGaAs detectors and the measured properties of the ISR we have extended the results and estimated the uncertainties in the optical power range from -50 to +40 dBm.

2.- Integrating sphere radiometer design.

Figures 1 and 2 show the sphere radiometer design and the external aspect of the final device, respectively. It is composed of a Spectralon® integrating sphere and two detectors. The sphere has an internal diameter of 2-inches with 0.5-inch thick walls. Three ports have been opened in the sphere with 90° orientation between each other. The input port has a 3 mm -diameter aperture and a FC fibre connector. The other two ports are used to place the two detectors, a 5 mm diameter Si detector (EG&G model G JUDSON UV-250B) and a 3 mm diameter InGaAs detector (Epitaxx ETX 3000). Two different BNC connectors, labeled ISR-Si and ISR-InGaAs provide the signal of the Si and InGaAs detectors respectively. Several adapters have been designed in order to ensure, by changing the distance fibre/sphere, that the maximum irradiance on the sphere wall does not overcome 1.7 W/cm^2. This maximum irradiance level was chosen to avoid optical damage in the Spectralon® surface.

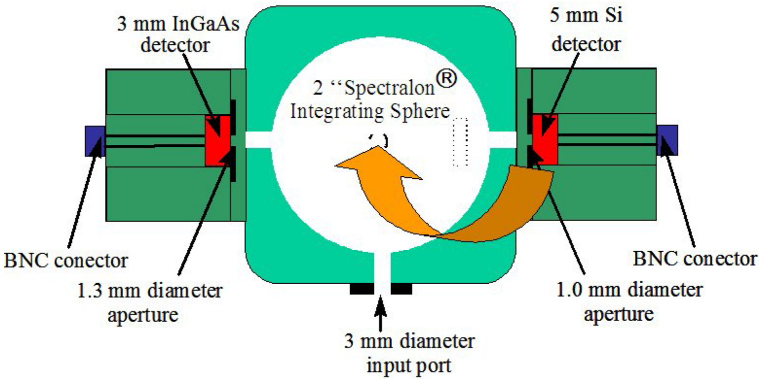

Figure 1: Integrating sphere radiometer (scheme).

Figure 2: Integrating sphere radiometer.

3.- Integrating sphere radiometer characterisation.

The radiometer characterization has been carried out by measuring the temperature coefficients and the linearity of the detectors before being attached to the sphere. The spatial non-uniformity, the spectral absolute responsivity and the connector effect were measured once they were adapted to the sphere.

3.1.- Coefficient of temperature

The temperature coefficient of the Si and InGaAs detectors were measured at two different temperature values (20º, 30ºC). The temperature coefficient of the Si detector oscillates between -0.06%/ºC at 400 nm to +0.03%/ºC at 900 nm. The InGaAs detector shows a temperature coefficient of less than +0.02%/ºC between 1000 and 1650 nm and +0.2%/ºC between 800 and 1000 nm.

3.2.- Linearity

The linearity of the sphere radiometer depends basically on the linearity of the detectors. In particular, Si and InGaAs detectors are highly linear when they are illuminated within their active area [9]. In order to ensure illumination within the collection ring of the detector, two apertures of 1.0 and 1.3 mm of diameter have been placed just in front of the Si and InGaAs detectors respectively. These apertures operate as attenuators without any kind of wavelength dependency. Additionally, the size of the apertures has been designed so as to avoid saturation of the detectors for 10 W of input power.

In order to evaluate the residual non-linearity in this configuration, we have measured the linearity of the detector and aperture sets in the same disposition as they are placed in the radiometer. We used a radiation of high numerical aperture to simulate the output port of the sphere. The superposition method described in [9] was used to measure the linearity over the full range of the InGaAs detector at 1550 nm. Based on the results of Boivin [6], the linearity of InGaAs detectors remains essentially the same in the range from 1200 nm to 1650 nm.

Figures 3 and 4 show the non-linearity of the detectors and its uncertainty (k=2) for both Si and InGaAs detectors, before being attached to the sphere radiometer. In the upper axis of these figures we represent the equivalent power level in the ISR calculated with their responsivities at 632.8 and 1550 nm respectively. The insets of both figures show the saturation levels estimated for the radiometer, 43.2 dBm for the ISR-Si (9.36 mA in the photodiode current) and +38.5 dBm for the ISR-InGaAs (6.46 mA in photodiode current). The maximum nonlinearity found in the range between -50 and +30 dBm was +0.01 dB, with an uncertainty of 0.022 dB (0.394%, k=2) in the ISR-Si, and -0.013dB, with an uncertainty of 0.016 dB (0.36 %, k=2) for the ISR-InGaAs.

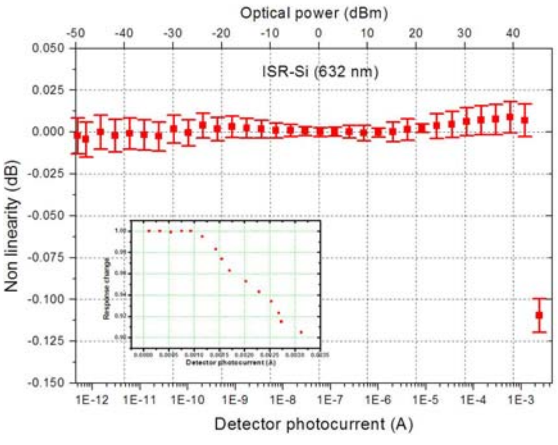

Figure 3: Linearity of the ISR-Si . The inserted figure shows the behaviour near the saturation point.

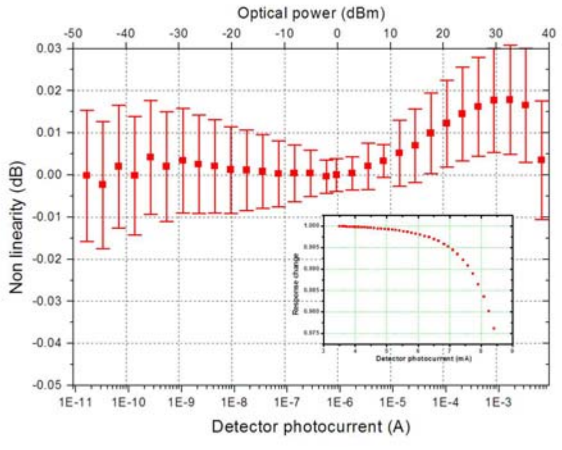

Figure 4: Linearity of the ISR-InGaAs. The inserted figure shows the behaviour near the saturation point

3.3.- Spatial non-uniformity of response

The spatial uniformity of the radiometer has been measured for the two detectors (ISR-Si and ISR-InGaAs) using collimated light. For the Si detector a He-Ne laser was used as the source while for the InGaAs detector a 1550 nm laser diode was employed. Figures 5 and 6 show the results obtained in both cases . The 1/e^2 beam waist used in the experiment was 1.2 mm, so that 99% of the power remained within a spot of 1.75 mm of diameter. In this area the standard deviation of the mean of the obtained responsivity values is 0,033% for the ISR-Si and 0,029% for the ISR-InGaAs.

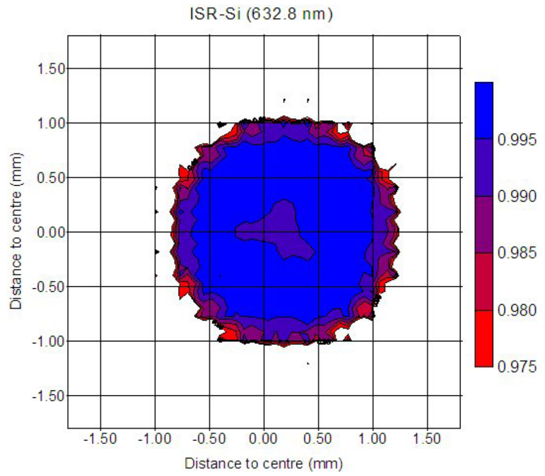

Figure 5: Spatial non-uniformity of response for Si detector.

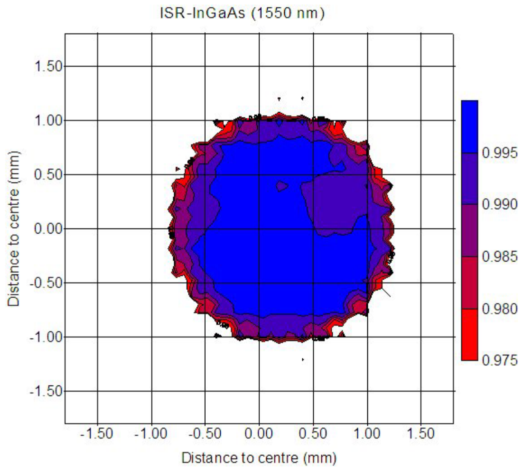

Figure 6: Spatial non-uniformity of response for ISR-InGaAs

3.4.- Absolute spectral responsivity measurement.

The absolute spectral responsivity calibration of the ISR has been performed by direct comparison with an Electrically Calibrated Pyroelectric Radiometer (ECPR) model RsP 590 with RS5900 display, manufactured by Laser Probe Corp., USA [10]. This ECPR radiometer is traceable to our absolute cryogenic radiometer [7]. Four tunable laser diodes covering the range between 1250-1650 nm were used in a calibration setup similar to the one used in reference [12]. At 850 nm a multimode laser diode has been used. For the visible range we used the emission lines of an Ar and a He-Ne laser.

The beam spots were within 1.3 ± 0.2 mm at $1/e^2$ irradiance diameter for all cases. An aperture of 3 mm diameter was used in the ECPR in order to minimize the scattered light. 1 mW optical power was used for all the measured wavelengths and this value was controlled by a monitor detector. Figure 7 shows the spectral responsivity and its uncertainty (k=2) obtained as result of the described process. Some inconsistencies in the results of the spectral responsivity have been found for wavelengths lying between 1340 to 1440 nm due to water absorption.

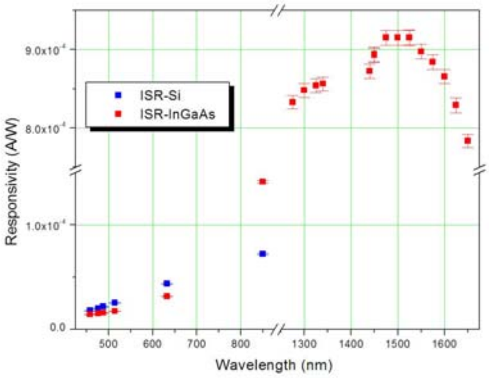

Figure 7: Spectral relative responsivity of the radiometer in the water vapour absorption region.

Table 1: Error due to connector effect.

Wavelength (nm)	R(λ)	σ	%
850	1.412E-04	3.43E-07	0.24
1300	8.480E-04	2.20E-06	0.26
1475	9.152E-04	2.38E-06	0.26
1550	8.975E-04	2.33E-06	0.26
1625	8.290E-04	2.38E-06	0.29
Medium value (%)			**0.26**

3.5.- Effect of the connector and numerical aperture

We have studied the variation of the ISR responsivity for different connectors and adapters determining different numerical apertures. To measure this variation, the sphere was calibrated by comparison with another integrating sphere radiometer. Table 1 shows the results at 850, 1300, 1477, 1550 and 1625 nm and the standard deviation of the mean obtained.

4. Uncertainty budget for the sphere radiometer calibration.

The sources of uncertainty identified in the calibration of the sphere radiometer are related to the transfer standard (ECPR), the characteristics of the sphere radiometer and the calibration setup. The contributions of the different sources of error to the final calibration uncertainty of the radiometer are summarized in Table 2. The uncertainties related to the ECPR radiometer are the calibration constant uncertainty, traceable to our absolute cryogenic radiometer [7], the spatial uniformity, the resolution of the radiometer display and the type A uncertainty estimated from six independent measurements. Additionally, to use the ISR, a picoamperimeter is needed (in our case the VINCULUM SP045) for which the resolution, gain, drift and type A uncertainties have been considered. Finally, the contribution to the uncertainty of the radiometer characterization, the temperature coefficient, the linearity, the spatial non-uniformity and the connector effect have been considered. The results obtained show a total expanded uncertainty lower than ±1.5 % (k=2) in all the useful wavelength range and for power levels from -50 dBm to +40 dBm.

Table 2: Uncertainties in the calibration of the integrating sphere radiometer with the ECPR.

Source of error	ISR-Si	ISR-InGaAs
	Valour (%)	Valour (%)
ECPR calibration constant	0.200	0.200
ECPR power measurement	0.100	0.100
ECPR resolution	0.020	0.020
ECPR wavelength response	0.165	0.165
ECPR spatial uniformity)	0.100	0.100
ISR current measurement	0.200	0.200
ISR resolution)	0.030	0.030
Picoamperimeter calibration	0.025	0.025
Picoamperimeter drift	0.020	0.020
ISR spatial uniformity	0.033	0.029
ISR temperature coefficient	0.240	0.080
Connector effect (ISR)	0.260	0.260
ISR linearity (-50 dBm a 40 dBm)	0.495	0.360
Relative standard uncertainty (k=2)	1.416	1.156

5.- Conclusions.

We have described the design, construction and characterization of a sphere radiometer useful for laser and optical fibre power meter calibrations. The radiometer is uses two different detectors (Si and InGaAs) so that it covers the wavelength range between 400 and 1700 nm. The calibration was done by direct comparison with an electrically calibrated piroelectric radiometer. Using the linearity factors of the detectors, we extend the radiometer calibration up to +40 dBm, with an estimated uncertainty lower than ±1.5 % (k=2) in the full spectral range.

Acknowledgements

We acknowledge financial support from the Ministerio de Educación y Ciencia (project TIC2003-01869 and the associated FPI grant), and the support of the Social European Fund through the grant program I3P of the CSIC)

References

[1] SRG Hall, TCE Jones, AG Roddie, “Traceability For High Power Fibre Optic Measurements” in *6th Optical Fibre Measurement Conference (OFMC’01 Proceedings.)* NPL, Teddington, Middlesex, UK, 2001, pp 77-80.

[2] I. Vayshenker, S. Yang, X. Li, T. R. Scott, C. L. Cromer, “Optical Fibre Power Meter Nonlinearity Calibrations at NIST”, NIST Special Publication 250-56 (2000).

[3] D. H. Nettleton, “Application of absolute radiometry to the measurement of optical power in fibre optic systems”, *New developments and applications in optical radiometry*. (Techno House, Bristol, UK, 1989), pp. 93-97.

[4] P. Corredera, J. Campos, M. L. Hernanz, J. L. Fontecha, A. Pons and A. Corróns. “Calibration of near-infrared transfer standards at optical fibre communication wavelengths by direct comparison with a cryogenic radiometer”. Metrologia **35**, 273-277 (1998).

[5] J. Envall, P. Kärhä and E. Ikonen. “Measurements of fibre optic power using photodiodes with and without an integrating sphere “. Metrologia **41**, 353–358 (2004).

[6] L. P. Boivin. “Properties of sphere radiometers suitable for high-accuracy cryogenic-radiometer-based calibrations in the near-infrared”. Metrologia, **37**, 273-278 (2000).

[7] P. Corredera, M. L. Hernanz, J. Campos, A. Corróns, A. Pons and J.L. Fontecha. “Absolute power measurements at wavelengths of 1300 nm and 1550 nm with a cryogenic radiometer and a tuneable laser diode”. Metrologia **37**, 513-516 (2000).

[8] P. Corredera, M. L. Hernanz, M. González-Herráez and J. Campos. “Anomalous non-linear behaviour of InGaAs photodiodes with overfilled illumination”. Metrologia, **40**, 150-153 (2003).

[9] IEC 61316. “Calibration of fibre-optic power meters”, Second Edition. 2004

[10] W. M. Doyle, B. C. McIntosh and J. Geist. “Implementation of a system of optical calibration based on pyroelectric radiometer”. Optical Engineering **15**, 541-548 (1976).

[11] P. Corredera, M. L. Hernanz, J. Campos, A. Corróns, A. Pons and J.L. Fontecha. “Comparison between absolute thermal radiometers at wavelengths of 1300 nm and 1550 nm“. Metrologia **37**, 543-546 (2000).

[12] Foukal P.V., Hoyt C., Kocchling H. and Miller P. “Cryogenic absolute radiometers as laboratory irradiance standards, remote sensing detectors, and pyroheliometers “ Appl. Opt. **29**, 983-993 (1990).